https://doi.org/10.1016/j.conbuildmat.2020.122103

Stress-Strain Behaviour of Cement-Stabilized Hong Kong Marine Deposits

by

Tsz-On Ho (PhD Candidate)
Department of Civil and Environmental Engineering
The Hong Kong Polytechnic University, Hung Hom, Kowloon, Hong Kong, China
Email: 16901171r@connect.polyu.hk

Wen-Bo Chen (Research Assistant Professor, Corresponding author)
Department of Civil and Environmental Engineering
The Hong Kong Polytechnic University, Hung Hom, Kowloon, Hong Kong, China
Tel : +852-3400 8075, Email: geocwb@gmail.com

Jian-Hua Yin (Chair Professor)
Department of Civil and Environmental Engineering,
The Hong Kong Polytechnic University, Hung Hom, Kowloon, Hong Kong, China
Email: cejhyin@polyu.edu.hk

Pei-Chen Wu (PhD Candidate)
Department of Civil and Environmental Engineering,
The Hong Kong Polytechnic University, Hung Hom, Kowloon, Hong Kong, China
Email:peichen.wu@connect.polyu.hk

and
Daniel C.W. Tsang (Associate Professor)
Department of Civil and Environmental Engineering
The Hong Kong Polytechnic University, Hung Hom, Kowloon, Hong Kong, China
Email: dan.tsang@polyu.edu.hk

Revised manuscript submitted to *Construction and Building Materials* for possible publication as a *research paper*
Dec. 2020

Abstract

The deep cement mixing (DCM) technique is an in-situ ground improvement method to stabilize and solidify soft clay ground. To facilitate the practical design of DCM, it is necessary to establish the relationship between the strength and stiffness of cement treated soil with governing factors first. In this study, the influence of different seawater and cement contents on the strength and stiffness of cement stabilized Hong Kong marine deposits (HKMD) was investigated by a series of unconfined/confined compression tests. According to the experimental results, an attempt was made to predict the unconfined compressive strength (UCS), q_u, by using a simple empirical equation based on water/cement ratio (w/c). The correlation between the strength and secant modulus of improved HKMD was obtained. Importantly, a linear relationship between small-strain (ε < 0.1%) stiffness and q_u was formulated based on the measurement results from local linear variable differential transformers (LVDTs) and strain gauges. Besides, the effect of w/c on the failure mode of the specimens was revealed. In addition, the consolidated undrained (CU) triaxial tests indicated that specimens gained higher peak strength with increase of confining pressure. All the findings are of practical significance for the local ground improvement industry as well as for other coastal cities around the world.

Keywords: deep cement mixing, ground improvement, Hong Kong Marine Deposits, stress-

strain behaviour, small-strain measurement.

Introduction

In recent years, the deep cement mixing (DCM) method has become an increasingly popular technique to strengthen reclaimed ground [1-4]. Initially developed in Japan and the Nordic countries in the 1970s, the DCM method is frequently employed to support embankments built on soft soil in Japan, Singapore, Thailand and many other countries [5-8], and has been adopted in reclamation projects of Hong Kong, e.g. the Third-runway System Project at the Hong Kong International Airport and the Tung Chung New Town Extension Project [9, 10], which utilization is likely to continue for soft soil foundation improvement in the foreseeable future.

Compared with other ground improvement techniques, the DCM method has relatively less adverse effects on the environment, because of involving an in-situ admixture stabilization technique in which a blade is pushed into the ground and cementing agents, then, are blended with soft ground. Such treated ground gains strength over a short period, thereby enhancing the bearing capacity, reducing the period of ground consolidation and decreasing the post-construction settlement. Compared with jet grouting, an alternative approach to introduce cement into the ground, by pressing air and water to cut and mix the soil under a relatively high pressure during installation [11], the DCM method causes less disturbance to the surrounding soil and reduces the uncontrolled soil movement in the adjacent ground. The mechanism of stabilizing soil by cement consists of four steps namely the hydration of binders, ion exchange reaction, formation of cement hydration products, and formation of pozzolanic reaction products [5]. The behaviour of strength [12, 13] and stiffness [14, 15] of cement stabilized soil have been extensively investigated over the past decades. A number of studies have been conducted and enable the prediction of the unconfined compressive strength (UCS) based on water/cement ratio (w/c) [2, 16-19]. However, relatively few reports are made on the whole picture of stress-strain behaviour from small ($\varepsilon < 0.1\%$) to large strain. The conventional measurement method, with which the axial strain of specimens is determined based on the relative movement between top and bottom loading platens, possibly introduces seating errors, alignment errors, bedding errors and compliance errors into the accurate deformation measurement [20, 21], especially within the small-strain region. Due to these errors, the stiffness of the specimen is much lower than its counterpart in the field condition [22]. Besides, the correlation between the small- or large- strain stiffness and strength of cement stabilized soft soil is of great practical significance.

As the mineralogy, deposition process, particle size distribution and climatic conditions of soft soil vary from place to place, a concern is often about the adoption of the empirical correlation acquired elsewhere for the local application. The soft clay used in this study is Hong Kong marine deposit (HKMD) that is one typical type of inorganic marine clay with high plasticity and its main clay minerals are kaolinite and illite, both of which are the main reactants in the pozzolanic reaction for the formation of additional calcium silicate hydrates and calcium aluminate hydrates [23-25]. Moreover, the locally obtained seawater was adopted in mixture in this study to well represent the reclamation project condition. Therefore, the results from this study are of practical significance for the engineering properties of other high plasticity inorganic clays with similar clay minerals. This paper presents the key results of stress-strain behaviour of laboratory prepared cement stabilized HKMD for both unconfined compression (UC) tests and consolidated undrained (CU) triaxial tests. The key aim is to propose an empirical formula to predict the strength of cement mixed HKMD. Importantly, the stiffness of cement stabilized HKMD specimens was measured by both global and local strain transducers in UC tests, to establish a correlation between small-strain ($\varepsilon < 0.1\%$) stiffness and the most widely measured unconfined compressive strength, q_u. In addition, the failure mode of specimens with different water/cement ratios were discussed.

Testing Materials and Methodologies

HKMD

The HKMD, used in this study, was taken from the seabed near Lantau Island in Hong Kong.

The physical properties of HKMD including the specific gravity, plastic limit W_p, liquid limit W_L, *pH* value, loss of ignition and particle size distribution are listed in Table 1. The chemical compositions of the HKMD are shown in Table 2.

Cement

The cement used to form the testing specimens in this study is ordinary Portland cement (OPC). To ensure the consistency of composition, the cement used, was taken from the same production batch. The chemical compositions of the cement thereby used, are shown in Table 3.

Nature Seawater

Since the DCM technique simulated a marine ground improvement technique, nature seawater was used to prepare the DCM columns (rather than distilled water) to reduce experimental discrepancy from the field conditions [26]. The nature seawater was taken from near coast of Chek Lap Kok in Hong Kong, which the pH and salinity are 7.92 and 32.241 g/L respectively, The detail of ion concentration of the nature seawater are shown in Table 4 conducted by ion chromatography (IC) tests [27].

Mixing design

Miura *et al*. [28] proposed that water/cement ratio, *w/c*, as a control variable for cement-stabilized clay, which is the ratio of initial water content, *w* (m_w/m_s), to the cement content, *c* (m_c/m_s), both of which are in terms of the dry mass of soil. Despite the common usage of DCM as a ground improvement method, no dosage methodologies have been developed based on a standardized procedure. Previous studies usually formulated the mixing design at a high initial water content, which was normally higher than 100% [11, 29, 30]. In order to obtain the same value of *w/c*, the water content of the HKMD and cement content could be verifying either or both. In addition, *w/c* was kept at 2.67 to 5, given the mixing difficulties and homogeneity of specimens in this study. The water content of the HKMD, during mixing, was adjusted to be between 80% to 120%, which is 1.5 to 2 times that of the liquid limit. Yin [31] concluded that no significant improvement was achieved when the cement content was lower than 5% and suggested that the cement content should be higher than 10%. The water and cement contents in the study are considered based on the ranges encountered in practical deep cement mixing projects. Therefore, the lowest cement content of 16% and the highest of 33.33% have been adopted in this study. The proposed mix design is presented in Table 4.

Specimens preparation

Lee *et al*. [2] found out that the process of drying and subsequent crushing the clay samples would lead to a significant reduction in the Atterberg limits and lowered the activity of the clay. The nature water content of HKMD was measured. The HKMD were mixed with extra seawater to achieve the targeted initial water content so as to avoid drying and crushing. Then, dry OPC powder was weighed and mixed with HKMD using a conventional concrete mixer for 5 mins. After thorough mixing, the cement-soil paste was cast in a cylindrical mould with an inner diameter of 50 mm and a length of 100 mm (a ratio of 1:2). The mould was firstly cleaned and the inner surface was coated with oil for easy demoulding. The mixture was placed, each time, up to one third of the height of mould and compacted dynamically by a falling hammer for ten strikes. The filled mould was placed on a vibration table for ten seconds to eliminate the air voids. A palette knife was used to trim the cement-soil mixture to ensure the surfaces of specimens were smooth. The specimens were wrapped in a polypropylene sheet to keep them moist until demolding. After 24 hours, the specimens were demolded and cured in a chamber with a relative humidity of 95% and a temperature of 25°C for . The curing period may be selected from 1, 3, 7, 14, 28 and 91 days, *etc*., depending on the purpose of test and the type of binder. 7 and 28 days are most commonly chosen [5, 19] so that the test results in this study can be easily compared with those reported by other researchers. Importantly, the 28-day unconfined compressive strength is a design parameter of the DCM improved soil ground [1]. Therefore, the curing time of 28 days was selected in this study. After curing was completed, the top and bottom surfaces of each specimen were ground, using the grinding machine to meet the requirements of perpendicularity, flatness and parallelism before testing. Additionally, weight and dimensions of the specimens were measured.

Unconfined Compressive (UC) test

The UC test of the specimens was performed using a VJ-Tech Tri-Scan 50 triaxial test machine at a fixed strain rate of 1mm/min. According to Horpibulsuk *et al.* [32], in each set of UC test, the stress-strain response and maximum strength developed will exhibit the similar pattern and level. The post-peak response is also of the similar pattern and residual stress will start to occur when strain reaches 3 to 4 %. Therefore, the maximum strain was capped at 5% in order to capture the overall profile of the stress-strain response of the specimens. Fig. 1 illustrates the overall view of the setting up. A load cell was fixed at the top of the triaxial machine to measure the axial loading, acting on the specimens. A 50 mm linear variable differentiate transformer (LVDT) was used to measure the global vertical strain, and two 5 mm LVDTs were fixed at the middle height of the specimens with the help of the mounting brackets to measure the local vertical strain. The procedure of installing the strain gauge followed the TML strain gauge guideline [33]. Before placing the strain gauge on the specimen, the DCM specimens were checked whether the mid-height surface is smooth and fully dry. To make sure good measurement performance of strain gauge, the surface should be precoated by PS adhesive if it is uneven. The precoating agents are TML strain gauge adhesive drug A-PS and drug B-PS-RP-2 which especially cater to strain gauges for concrete or mortar. The mixed PS adhesive coating layer is 0.5 mm to 1 mm in thickness. After the PS adhesive fully dried, CN adhesive was used to adhere the strain gauge to specimen surface precoated with PS adhesive. Two 5 mm×30 mm strain gauges were used to measure the vertical strain and two 5 mm×30mm strain gauges for the radial strain. According to the interim guideline 2017 [34], the axial compressive stress is calculated from the following equation

$$\sigma_1 = \frac{P(1-\varepsilon)}{A_o} \times F \quad (1)$$

where P is the force applied to the specimen for each set of readings; ε stands for the axial strain of the specimen for each set of readings; A_0 presents the initial cross-sectional area of the specimen and F refers to the strength correction factor. Since all specimens reached unconfined compressive strength (UCS) at axial strain ranging from 1% to 1.5% accompanying by a brittle failure manner, area correction is not as critical as that in soil. Therefore, it was considered that area correction was not required for determining the peak strength [34].

Consolidated Undrained (CU) triaxial compression test

The VJ-Tech Tri-Scan 50 triaxial apparatus was used to conduct the CU triaxial test by following the British Standard BS1377 [35]. Before being installed in the triaxial apparatus, all the specimens were soaked in distilled water in a container with vacuum pressure. Side filter paper strips were placed on the surface of the specimens to speed up consolidation. The back pressure was increased gradually to 200 kPa to ensure a saturation degree of higher than 95%. The isotropic consolidation pressures of 100, 200, 300 and 400 kPa were adopted in this study. The shearing rate was 0.2 mm/min which was the same as that used by Yin and Lai [36]. The compression normally was normally stopped once axial strain reached up to 15%.

Results and Discussions

Unconfined Compression (UC) Tests

Table 5 summarizes the mixing design of cement mixed HKMD at a *w/c* ratio of 2.67 to 5 after 28 days of curing. The UCS of all mixing proportions ranged from 0.8 to 1.4 MPa. The water content for mixing was kept constant at 80%, 100% and 120% respectively, while only the cement content varied so that the *w/c* was at 3, 4 and 5 for each level of water content. It was observed that the q_u increased with the increase of cement content when the water content was kept at 100% and 120%. However, the increase cement content had no impact on UCS when the water content was kept at 80%, possibly suggesting that the DCM method was not effective in increasing strength when the water content was below a certain level. Similarly. Chew *et al.* [23] found that strength gain would slow down when cement content increased to certain level. The occurrence of this phenomenon was dependent on the initial water content of DCM samples. Fig. 2 shows the typical stress-strain curves of the specimens with a cement content of 25% and a water content of 100% (*i.e.* w/c = 4). The enlarged graph shows that the measurement results from local LVDTs and local strain gauges matched well with each other. Besides, it can be observed that global strain was significantly larger than local strain, which can be possibly explained by the sitting errors, bedding errors and compliance errors when vertical strain was determined by global LVDT [37, 38]. This typical curve also confirmed the above-mentioned statement that q_u usually appears where strain was between 1% and 1.5%. Additionally, local LVDTs and strain gauges failed to measure the strain after specimen failure occurred. It is also noted that the specimens presented significant strain softening behavior, which showed the combined effect of cement and soft clay, because of the unconfined condition in UC tests. More contents are discussed about reduction of the strain softening behaviour by providing confining pressure.

Strength of cement stabilized HKMD

Horpibulsuk *et al.* [16] proposed an exponential function based on Abrams' law, which is commonly used for modeling the strength of cementitious materials. A power function in the form of $y = ax^{-b}$ was currently used as the fitting equation here. Fig. 3 illustrates the influence of *w/c* on q_u. The data was presented together with the results of the cement mixed HKMD from Yin and Lai [36]. The average value of each set of unconfined compressive strength values were adopted for fitting the power function in figure. The correlation coefficient R^2 was higher than 0.95, indicating a satisfactory correlation. The equation of curves is shown as follows:

$$q_u = 5.35\left(\frac{w}{c}\right)^{-1.09} \tag{2}$$

The *w/c* is the most influential factor in the strength prediction equation. The current results were in good agreement with the results presented by Yin and Lai [36], sourced from a coastal area near Tai Kwok Tsui Harbour in Hong Kong.

Given the above, it strongly appears that using *w/c* ratio to govern the design of deep cement mixed soil can be a reliable approach. It was observed that mix design can be formulated in accordance with the accurate determination of the natural water content of soil, which was consistent with the hypothesis made by Miura *et al*. [28]. This was not true in the present study where corresponding *w/c* ratio was lower than 3 when water content was 80%, which reached only half of the expected value and hence possibly suggested that mixing water content had an optimum value.

Fig. 4 shows the comparison between the strength of cement stabilized clay results gathered from different Asian countries, including the results from the current study and the test result from the HKMD by Yin and Lai [36], Singapore Maine clay [2], Bangkok clay [16] and Japanese Arake clay [17]. It should be noted that all kinds of cement stabilized clay in the above studies had a curing period of 28 days. Different types of clay led to similar results, showing that the *w/c* was a dominant parameter influencing the engineering behaviour of cement stabilized clay, because of different clay conditions such as plasticity index. The limitation of the above relation is that the variation in curing time cannot be accounted for directly. The UCS increased with the decrease of *w/c*. However, it can be reasonably speculated that q_u cannot further increase with the further decrease of *w/c*, indicating that a minimum *w/c* value should exist to get the highest UCS.

Secant Modulus, $E_{sec,50}$ and $E_{sec,i}$,*- global LVDT, local LVDT and strain gauges*

The $E_{sec,50}$ and $E_{sec,i}$ are defined as follows:

$$E_{sec,50} = \frac{q_{50}}{\varepsilon_{50}} \quad (3)$$

where q_{50} is 50% of ultimate stress and ε_{50} represents the axial strain corresponding to q_{50} and, determined from the stress-strain curve.

and

$$E_{sec,i} = \frac{q_i}{i} \quad (4)$$

where i is a specific axial strain and q_i refers to the corresponding stress at the strain of i. Fig. 5 shows the diagram of the calculation methods of secant modulus, $E_{sec,50}$ and $E_{sec,i}$ from the stress-strain curve. Fig. 6 shows the relationship between the secant modulus, $E_{sec,50}$ and UCS, q_u, which is a common practice to correlate the two parameters. It is of practical significance for engineers to calculate the value of secant modulus by measuring q_u. The $E_{sec,50}$ determined by global LVDT entirely fell into the range from 70 to 239q_u (The best fitting line was 125.07q_u), which was slightly higher than 89q_u presented by Yin [31] and similar to those reported by Tan *et al.* [1] (*i.e.* 150q_u to 400q_u). Additionally, the $E_{sec,50}$ determined by local strain measurement using the strain gauges varied from 504 to 1075q_u (The best fitting line was 765.94q_u). The results of the $E_{sec,50}$ using local strain measurements were much higher than those using global strain measurement. The modulus, using the conventional global axial-displacement measurement, was largely underestimated. It was comparable with the result reported by Tan *et al.* [11] (*i.e.* 350 to 800q_u) and Tatsuoka *et al.* [39] (*i.e.* 1000q_u) both of whom adopted a similar method when measuring local strain. However, it should be pointed out that the parameters of HKMD acquired should be verified for other types of soft clay due to the varying physico-chemical properties of soils from a variety of regions. Using q_u to calculate an accurate $E_{sec,50}$ *is* of importance to design and check the confined compression modulus of the final settlement of the improved foundation [1].

The variation of stiffness with the strain of cement stabilized HKMD specimens was found by plotting the results in terms of E_{sec} versus log ε_a which refer to secant modulus and axial strain respectively. Fig. 7 shows a typical curve, with cement content of 25%, and water content of 100% ($w/c = 4$). The strain was measured by three types of transducers, which thus suggested that different transducers can measure different ranges of strain, strain gauges measure strain from 0.01% to 0.1%, local LVDTs measure strain from 0.01% to 1%, while global LVDTs are only suitable for measuring strain which is larger than 0.5%. The curves from three transducers almost overlapped simultaneously at the same ranges of axial strain and constituted quite a smooth stiffness degradation curve, indicating that good reliability was achieved by these three strain measurement techniques. Fig.7 shows that the cement stabilized HKMD seems to behave non-linearly at small strain. The small strain behavior was more akin a very stiff clay.

To further analyze and discuss the stress-strain relationship of cement stabilized HKMD, linear relationships are found between the q_u and the secant modulus at different strain levels, as shown in Fig. 8. The best fitting equations were $E_{sec,1}$=93.29q_u, $E_{sec,0.1}$=615.51q_u and $E_{sec,0.01}$=905.27q_u. The coefficients of correlation, R^2 of the fitting equations were 0.91, 0.77 and 0.43, respectively. Since the precise measurement of small strain is challenging, error of measurement may occur. As shown in Figure 8(c), one abnormal data (circled data point) offsets the fitting line obviously. If a new fitting curve is fitted without the abnormal data point, the coefficient of correlation, R^2 will be increased to 0.64 and the best fitting equation is $E_{sec,0.01}$ = 888.36 q_u. The strain with strain level smaller than 0.01% is largely elastic, the compressive strength, however, is a gradual compression process with significantly progressive plastic strains. It is suggested the relationship between $E_{sec,0.01}$ and q_u obtained here can be a reliable reference in practical projects after careful considerations.The reducing trend of correlation coefficients with decreasing axial strain can be explained by a larger noise in the measurement of smaller strain, thereby inducing a larger scatter in the data. The stiffness ratio of the $E_{sec,1}$ and $E_{sec,0.1}$ were 0.152 and the ratio of the $E_{sec,1}$ and $E_{sec,0.01}$ were 0.103. $E_{sec,i}$, modulus at small strain, can be obtained and related to strain and q_u was of importance for routine design. Due to the difficulty in achieving and measuring stiffness accurately in routine laboratory testing, most of the tests revealed that stiffness was far lower than that inferred from field behavior [40]. Therefore, it is important to explicitly capture small-strain behaviour [19, 41]. The secant modulus increased almost linearly with both q_u. The small strain of cement stabilized HKMD can be easily predicted by using q_u.

Failure modes of cement stabilized HKMD specimens

Typically, three kinds of failure modes were observed, namely cone-split, columnar, and shear fracture patterns all of which were very similar to those of cylindrical concrete specimens classified by ASTM C39/C39M [42] (types 2, 3 and 4). Fig. 9 shows the typical failure pattern of the cement stabilized HKMD specimens after UC tests. Fig.9(a) shows the specimen with shear failure that was a diagonal facture without cracks at both ends. Fig.9(b) shows that the failure pattern is in the form of a cone-split facture was well formed at only one end and with vertical cracks running through the caps. Fig. 9(c) shows the specimen failure with columnar factures which vertical cracking through both ends. The failure mode shifted from random fracturing to prominent shear failure, due to the increase in water cement ratio, *w/c* shown in Fig. 10. The failure pattern was related to the strength of the specimens based on different water and cement contents. It was observed that cone-split and columnar factures were commonly observed form samples mixed at a high *w/c* ratio (*w/c* = 5 in this study), while shear failure was the major failure mode observed from samples with a low *w/c* ratio (*w/c* =3 and 4 in this study). The underlying mechanism can be possibly explained by the microcracks induced by hydration reaction and applied loading in the specimen. Estabragh *et al*. [43] indicated that shrinkage microcracks developed in the cement stabilized clay due to the loss of water content during drying or hydration reaction. The greater cement content was, the higher the amount of heat from hydration of cement would be, thereby inducing excessive microcracks. Under external applied loading, the excessive microcracks in the specimen with higher cement content were more prone to propagate and interconnect with each other, which well explaining the formation of clear shear bands and the mode of shear failure. However, the microcracks in the specimens with lower cement content were difficult to be interconnected so that a more brittle failure mode was commonly observed. Besides, Zhang *et al.* [44] indicated the cement stabilized soil exhibits much more ductile behavior when the mixture design with high salt concentration than cement stabilized soil with low salt concentration. Therefore, when *w/c* ratio increase, cement stabilized HKMD behaved more ductile and shear failure occur. It is an interesting issuer to be further identified the failure mode behaviors.

Consolidated Undrained (CU) triaxial tests

For the specimens with a *w/c* ratio of 4 and water content of 100%, the curves of the relationships between deviator stress-axial strain and pore pressure-axial strain under the confining pressures of 100 kPa, 200 kPa, 300 kPa and 400 kPa are shown in Figs. 11(a) and 11(b). The stress and strain used in this analysis are shown as follows:

$$q = \sigma_1^{'} - \sigma_3^{'} \qquad (5)$$

and

$$p' = (\sigma_1^{'} + \sigma_2^{'} + \sigma_3^{'})/3, \quad where \quad \sigma_2^{'} = \sigma_3^{'} \qquad (6$$

where σ_1' is the major principal effective stress, σ_2' and σ_3' represent two minor principal effective stresses, q stands for the deviator stress, p' refers to mean effective stress. The samples consolidated under higher confining pressure failed at greater deviator stress and strain. Fig. 11(a) shows that the confining pressure also helped to increase residual stress from 0.7 MPa to 1.1 MPa. The negative pore pressure of each specimen was observed, which shows the dilatant behaviour of all specimens presented in Fig. 11(b). A higher confining pressure was generally associated with larger volumetric strain while lower confining pressure led to the greater the degree of dilation. The effective stress paths of cement stabilized HKMD in the p'-q plane are depicted in Fig. 11(c).

Fig. 12(a) shows a normalized stress strain curve of cement stabilized HKMD demonstrates that strength has a clear increase with the increase of curing time from 28 to 200 days. The UCS increases from 1.5 to 2.5 MPa, and the strength ratio between the specimens after 200 days and 28 days of curing was 1.67 ($q_{u,200}/q_{u,28}$). A similar finding that the ratio of the specimens after 91 days and 28 days curing is 1.44 ($q_{u,91}/q_{u,28}$) was presented by Cement Deep Mixing Method Association [45]. The test results from the present study showed that the strength did keep increasing after 28 days of curing. Therefore, it can be deemed that using the strength after the curing of 28 days as a design parameter is over conservative. In addition, it can be seen from Fig. 12(b) that the secant modulus of the specimens also has a significant increase due to the increase in confining pressure and under higher confining pressure presents a lower decreasing rate.

Conclusions

A series of unconfined compression and consolidated undrained compression tests on cement stabilized HKMD specimens were conducted in this study considering varying water/cement ratios, cement contents, and confining pressures. The global and local measurement devices were adopted to measure the vertical strain of the specimens in different scales. Based on the current results and the subsequent analysis, the following findings and conclusions are presented:

(1) It is observed that the water/cement ratio, *w/c,* is the prime parameter influencing the engineering behaviour of cement stabilized HKMD. The correlation among UCS, $q_{u,}$ after 28 days of curing and *w/c* was proposed as $q_u = 5.35\left(\frac{w}{c}\right)^{-1.09}$. This relationship agrees quite well with the previous test results of HKMD in existing literature, even though the soils were obtained from two different sites. Hence, it is of practical significance for local

engineers.

(2) Due to the sitting errors, bedding errors and compliance errors, the external strain measurement method (global LVDT) shows a softer behaviour as compared to local strain measurement (local LVDT). In addition, the small strain behaviour of the cement stabilized HKMD are recognized to be nonlinear, more like a very stiff clay.

(3) The small-strain measurement of cement stabilized HKMD was conducted. The secant modulus, $E_{sec,i.}$ is observed to linearly increase with the UCS, q_u. The small strain of cement stabilized HKMD can be easily predicted by using q_u. Besides, easy-using stiffness ratio is obtained for routine design.

(4) The failure modes of cement stabilized HKMD specimens are influenced by *w/c* significantly. The failure mode converges to shear fracture pattern as *w/c* reduces.

(5) Last but not least, CU tests have showed that the deviator stress of the cement stabilized HKMD is larger under higher confining pressure. This study also confirms that the peak strength and stiffness of the cement stabilized HKMD keep increasing with time after 28 days of curing.

Acknowledgments

The work in this paper is supported by a Research Impact Fund (RIF) project (R5037-18), a Three-based Research Scheme Fund (TRS) project (T22-502/18-R), and three General Research Fund (GRF) projects (PolyU 152209/17E; PolyU 152179/18E; PolyU 152130/19E;) from Research Grants Council (RGC) of Hong Kong Special Administrative Region Government of China. The authors also acknowledge the financial supports from Research Institute for Sustainable Urban Development of The Hong Kong Polytechnic University and three grants (BBAG, ZDBS, ZVNC) from The Hong Kong Polytechnic University. Last but not least, the authors would like to take this opportunity to offer our sincere gratitude to Ms. Elaine Anson who polished the manuscript, Mr. Lo Chun Hang, who assisted to conduct and prepare the laboratory tests, as well as the editors and reviewers who provided meaningful comments.

References

[1] J.-H. Yin, Properties and behaviour of a cement mixed Hong Kong marine clay and design applications, In Proceedings of "Ground Treatment" of a seminar organised by HKGES, HKIE-GD and CityU, Hong Kong, (2004) 97-105.

[2] F.-H. Lee, Y. Lee, S.-H. Chew, K.-Y Yong, Strength and modulus of marine clay-cement mixes, J. Geotech. Geoenviron. 131.2 (2005) 178-186.

[3] H. Xiao, W.-H. Shen, F.-H. Lee, Engineering properties of marine clay admixed with Portland cement and blended cement with siliceous fly ash. J. Mater. Civil. Eng. 29(10) (2017) 04017177.

[4] S. Melentijevic, J. L. Arcos, C. Oteo, Application of cement deep mixing method for underpinning, In Proceedings of the 18th International Conference on Soil Mechanics and Geotechnical Engineering, (2013) 2549-2552.

[5] M. Kitazume, M. Terashi, The deep mixing method. CRC press, 2013.

[6] A. Porbaha, State of the art in deep mixing technology: part I. Basic concepts and overview, Proceedings of the Institution of Civil Engineers-Ground Improvement 2.2 (1998) 81-92.

[7] A. Porbaha, S. Shibuya, T. Kishida, State of the art in deep mixing technology. Part III: geomaterial characterization, Proceedings of the Institution of Civil Engineers-Ground Improvement, 4.3(2000) 91-110.

[8] A. Porbaha, State of the art in deep mixing technology. Part IV: design considerations.

Proceedings of the Institution of Civil Engineers-Ground Improvement 04(3) (2000) 111-125.

[9] P.-C. Wu, W.-Q. Feng, J.-H. Yin, Numerical study of creep effects on settlements and load transfer mechanisms of soft soil improved by deep cement mixed soil columns under embankment load, Geotext. Geomembranes 48.3 (2020) 331-348.

[10] T.-O. Ho, D.-C. Tsang, W.-B. Chen, J.-H. Yin, Evaluating the Environmental Impact of Contaminated Sediment Column Stabilized by Deep Cement Mixing, Chemosphere (2020) 127755.

[11] T.-S. Tan, T.-L. Goh, K.-Y. Yong, Properties of Singapore marine clays improved by cement mixing, Geotech. Test. J. 25.4 (2002) 422-433.

[12] T.-S. Nagaraj, N. Miura, P.-P. Yaligar, A. Yamadera, Predicting strength development by cement admixture based on water content, Geotechnical Engineering Bulletin 7.1 (1998).

[13] K. Uddin, A.-S. Balasubramaniam, D.-T. Bergado, Engineering behavior of cement-treated Bangkok soft clay, Geotechnical Engineering 28 (1997) 89-119.

[14] J. Asano, Deep mixing method of soil stabilization using coal ash, Proc. of IS-Tokyo'96, The 2nd International Conference on Ground Improvement Geosystems. (1996).

[15] S. Saitoh, Y. Suzuki, S. Nishioka, R. Okumura, Required strength of improved ground. Grouting and deep mixing: Proc. IS Tokyo ’96, 2nd Int. Conf. on Ground Improvement Geosystems (1996) 375– 380.

[16] S. Horpibulsuk, N. Miura, T.-S. Nagaraj, Assessment of strength development in cement-admixed high water content clays with Abrams' law as a basis, Géotechnique 53.4 (2003) 439-444.

[17] S. Horpibulsuk, N. Miura, H. Koga, T.-S. Nagaraj, Analysis of strength development in deep mixing: a field study, Proceedings of the Institution of Civil Engineers-Ground Improvement. 8.2 (2004) 59-68.

[18] K. Yao, Y. Pan, L. Jia, J.-T. Yi, J. Hu ,C.-Z. Wu. Strength evaluation of marine clay stabilized by cementitious binder. Mar. Georesour. Geotec. 38(6) (2020) 730-743.

[19] K. Yao, N. Li, D. H. Chen, W. Wang. Generalized hyperbolic formula capturing curing period effect on strength and stiffness of cemented clay. Constr. Build Mate. 199 (2019) 63-71.

[20] G.K. Scholey, J.D. Frost, D.L. Presti, M. Jamiolkowski, A review of instrumentation for measuring small strains during triaxial testing of soil specimens. Geotech. Test. J. 18 (2) (1995) 137-156.

[21] X. S. Shi, K. Liu, J.H. Yin, Effect of Initial Density, Particle Shape, and Confining Stress on the Critical State Behavior of Weathered Gap-Graded Granular Soils. J. Geotech Geoenviron, 147(2), (2020) 04020160.

[22] R.-J. Jardine, M.-J. Symes, J.-B. Burland, The measurement of soil stiffness in the triaxial apparatus, Geotechnique 34(3) (1984) 323-340.

[23] S.-H. Chew, A. H. M. Kamruzzaman, F. -H. Lee, Physicochemical and engineering behavior of cement treated clays, J. Geotech. Geoenviron. 130(7) (2004) 696-706.

[24] S. Horpibulsuk, R. Rachan, A. Chinkulkijniwat, Y. Raksachon, A. Suddeepong, Analysis of strength development in cement-stabilized silty clay from microstructural considerations, Constr. Build. Mater. 24(10) (2010) 2011-2021.

[25] Y. -J. Du, N.-J. Jiang, S. -Y. Liu, F. Jin, D. -N. Singh, A. J. Puppala, Engineering properties and microstructural characteristics of cement-stabilized zinc-contaminated kaolin, Can. Geotech. J. 51(3) (2014) 289-302.

[26] P. Li, W. Li, T. Yu, F. Qu, V. -W. Tam, Investigation on early-age hydration, mechanical properties and microstructure of seawater sea sand cement mortar, Constr. Build Mater. 249 (2020) 118776.

[27] J. -G. Teng, Y. Xiang, T. Yu, Z. Fang, Development and mechanical behaviour of ultra-high-performance seawater sea-sand concrete, Adv. Struct. Eng. 22(14) (2019) 3100-3120.

[28] N. Miura, S. Horpibulsuk, T.-S. Nagaraj, Engineering behavior of cement stabilized clay at high water content, Soils Found. 41(5) (2001) 33-45.

[29] J.-R. Jacobson, G.- M. Filz, J.- K. Mitchell, Factors affecting strength gain in lime-cement columns and development of a laboratory testing procedure, Virginia Center for Transportation Innovation and Research, 2003.

[30] S. Horpibulsuk, W. Phojan, A. Suddeepong, A. Chinkulkijniwat, M.-D. Liu, Strength

development in blended cement admixed saline clay, Appl. clay sci. 55 (2012) 44-52.

[31] J.-H. Yin, Stress-strain-strength characteristics of soft Hong Kong marine deposits without or with cement treatment, Lowland Technology International, 3.1, June (2001) 1-13.

[32] S. Horpibulsuk, N. Miura, T.S. Nagaraj, Clay – water / cement ratio identity for cement admixed soft clays. J. Geotech. Geoenviron. 131(2) (2005) 187-192.

[33] Tokyo Sokki Kenkyujo Co., TML strain gauge TML Pam E-1007C(2017).

[34] HKIE, Interim Guidelines on Testing of Unconfined Compressive strength of Cement Stabilized Soil Cores in Hong Kong, Hong Kong Institution of Engineers (2017).

[35] BSI, BS1377, Methods of test for soils for civil engineering purposes, British Standards Institution, Milton Keynes, UK (1990).

[36] J.-H. Yin, C.-K. Lai, Strength and stiffness of Hong Kong marine deposits mixed with cement, Geotechnical Engineering 29.1 (1998).

[37] G.-K. Scholey, J.-D. Frost, D.-L. Presti, M. Jamiolkowski, A review of instrumentation for measuring small strains during triaxial testing of soil specimens, Geotech. Test. J. 18.2 (1995) 137-156.

[38] W.-B. Chen, W.-Q. Feng, J.-H. Yin, L. Borana, LVDTs-based radial strain measurement system for static and cyclic behavior of geomaterials, Measurement 155 (2020) 107526.

[39] F. Tatsuoka, Y. Kohata, K. Uchida, K. Imai, Deformation and Strength Characteristics of

Cement-Treated Soils in Trans-Tokyo Bay Highway Project, Proceedings, IS-Tokyo96/2nd International Conference on Ground Improvement Geosystems, Tokyo: Vol. 1, (1996) pp. 453–459.

[40] J. H. Atkinson, Non-linear soil stiffness in routine design, Géotechnique, 50(5), (2000) 487-508.

[41] K.-K. Lu, J.-H. Yin, S.-C. Lo, Modeling small-strain behavior of Hong Kong CDG and its application to finite-element study of basement-raft footing, Int. J. Geomech. 18.9 (2018) 04018104.

[42] ASTM C39/C39M, Standard Test Method for Compressive Strength of Cylindrical Concrete Specimens (C39/C39M), ASTM International. West Conshohocken, PA. (2015).

[43] A. R. Estabragh, P. Namdar, A. A. Javadi, Behavior of cement-stabilized clay reinforced with nylon fiber, Geosynth. Int. 19(1) (2002) 85–92.

[44] D.-W. Zhang, L.-B. Fan, S.-Y. Liu, Y.-F. Deng, Experimental investigation of unconfined compression strength and stiffness of cement treated salt-rich clay, Mar. Georesour. Geotec. 31(4) (2013) 360-374.

[45] Cement Deep Mixing Method Association, Cement Deep Mixing Method (CDM), Design and Construction Manual (in Japanese) (1999).

Caption list of tables

Table 1. Physical properties of HKMD

	Specific Gravity	Liquid Limit (%)	Plastic Limit (%)	Plasticity Index (%)	pH Value	Loss of Ignition	Particle Size Distribution (%)		
							Sand	Silt	Clay
HKMD	2.60	59.3	27.5	31.8	7.11	4.31	3.5	77.5	19.0

Table 2. Chemical compositions of HKMD

Components	Na_2O	MgO	Al_2O_3	SiO_2	P_2O_5	SO_3	Cl	K_2O	CaO	TiO_2	MnO	Fe_2O_3	ZnO	Rb_2O	SrO	ZrO_2
Percentage (%)	1.24	2.63	21.80	58.00	0.12	2.10	0.79	3.42	2.63	0.84	0.08	6.30	0.01	0.02	0.02	0.03

Table 3. Chemical compositions of the cement

Components	SiO_2	Fe_2O_3	Al_2O_3	CaO	MgO	SO_3
Percentage (%)	20.00	3.04	5.53	64.30	1.28	4.49

Table 4. Chemical compositions of nature seawater in Chek Lap Kok [27]

Ion	F^-	Cl^-	Br^-	SO_4^{2-}	NO^{2-}	NO^{3-}	PO_4^{3-}	Li^+	Na^+	NH_4^+	K^+	Mg^{2+}	Ca^{2+}	Salinity
(g/L)	0.000	18.153	0.066	1.675	0.000	0.000	0.000	0.0007	10.419	0.000	0.354	1.215	0.358	32.241

Table 5. Summary of different mixture designs of unconfined compression tests and consolidated undrained triaxial tests

No.	Name[1]	Test types	Confining pressure, σ'_3 (kPa)	Water content, m_w/m_s (%)	Water/cement ratio, w/c	Cement content, m_c/m_s (%)
1	W80_wc 5_1					
2	W80_wc 5_2				5.00	16
3	W80_wc 5_3					
4	W80_wc 4_1					
5	W80_wc 4_2				4.00	20
6	W80_wc 4_3					
7	W80_wc 3_1					
8	W80_wc 3_2			80		
9	W80_wc 3_3				3.00	27
10	W80_wc 3_4					
11	W80_wc 3_5					
12	W80_wc 3_6					
13	W80_wc 2.67_1					
14	W80_wc 2.67_2				2.67	30
15	W80_wc 2.67_3					
16	W100_wc 5_1					
17	W100_wc 5_2	UC test	-		5.00	20
18	W100_wc 5_3					
19	W100_wc 4_1					
20	W100_wc 4_2					
21	W100_wc 4_3					
22	W100_wc 4_4			100	4.00	25
23	W100_wc 4_5					
24	W100_wc 4_6					
25	W100_wc 4_7					
26	W100_wc 3_1					
27	W100_wc 3_2				3.00	33
28	W100_wc 3_3					
29	W120_wc 5_1					
30	W120_wc 5_2				5.00	24
31	W120_wc 5_3			120		
32	W120_wc 4_1					
33	W120_wc 4_2				4.00	30
34	W120_wc 4_3					
35	W100_wc 5_1_100		100			
36	W100_wc 5_2_200	CU test	200	100	4.00	25
37	W100_wc 5_3_300		300			
38	W100_wc 5_4_400		400			

Note: 1. The designation 'W" refers to water content, and designation 'wc' refers to water/cement ratio.

Caption of figures

Fig. 1. Photo of detailed testing setup

Fig. 2. A typical stress-strain curve of unconfined compression test on a cement stabilized HKMD specimen using global and local axial strain measurement methods

Fig. 3. Plot of unconfined compressive strength of cement stabilized HKMD *versus* water/cement ratio

Fig. 4. Relationships between unconfined compressive strength of cement stabilized soils with water/cement ratio from different countries

Fig. 5. A schematic diagram of methods for calculating of $E_{sec,50}$ and $E_{sec,i}$ from stress-strain curve

Fig. 6. Plots of unconfined compressive strength *versus* $E_{sec,50}$ determined by using local and global axial strain measurement methods

Fig. 7. Typical secant modulus degradation curve based on the data from global and local axial strain measurement methods

Fig. 8. Plots of secant modulus (a) $E_{sec,1}$, (b) $E_{sec,0.1}$, and (c) $E_{sec,0.01}$ of specimens with its corresponding unconfined compressive strength, q_u

Fig. 9. Typical failure modes of cement stabilized HKMD specimens: (a) shear fracture, (b) cone and split fracture, (c) columnar fracture

Fig. 10. Percentage of different failure modes of cement stabilized HKMD specimens with different *w/c* ratios

Fig. 11. Plots of (a) deviator stress *versus* aixal strain, (b)excess porewater pressure *versus* axial strain,(c) effective stress paths in compression stage of the specimens with 25% cement content and 100% water content (*i.e. w/c*: 4) under different confining pressures

Fig. 12. Plots of (a) normalized stress-strain curve and (b) secant modulus *versus* axial strainof the cement stabilized HKMD specimen with 25% cement content and 100% water content (*i.e. w/c*: 4)

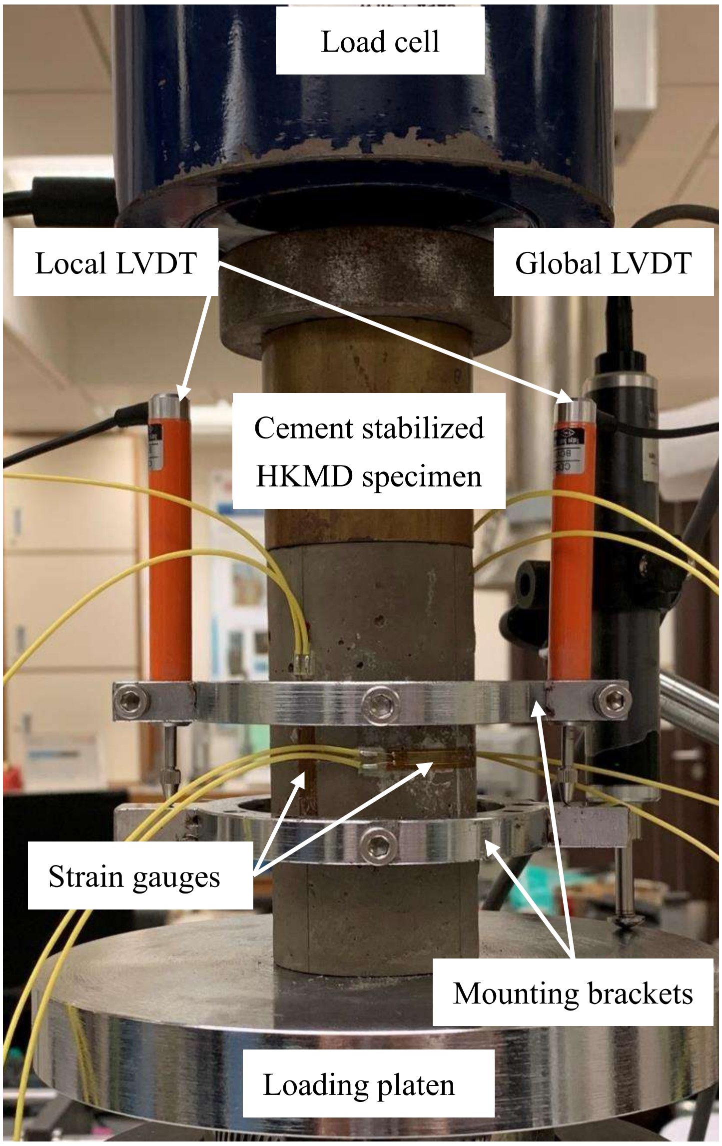

Fig. 1. Photo of detailed testing setup

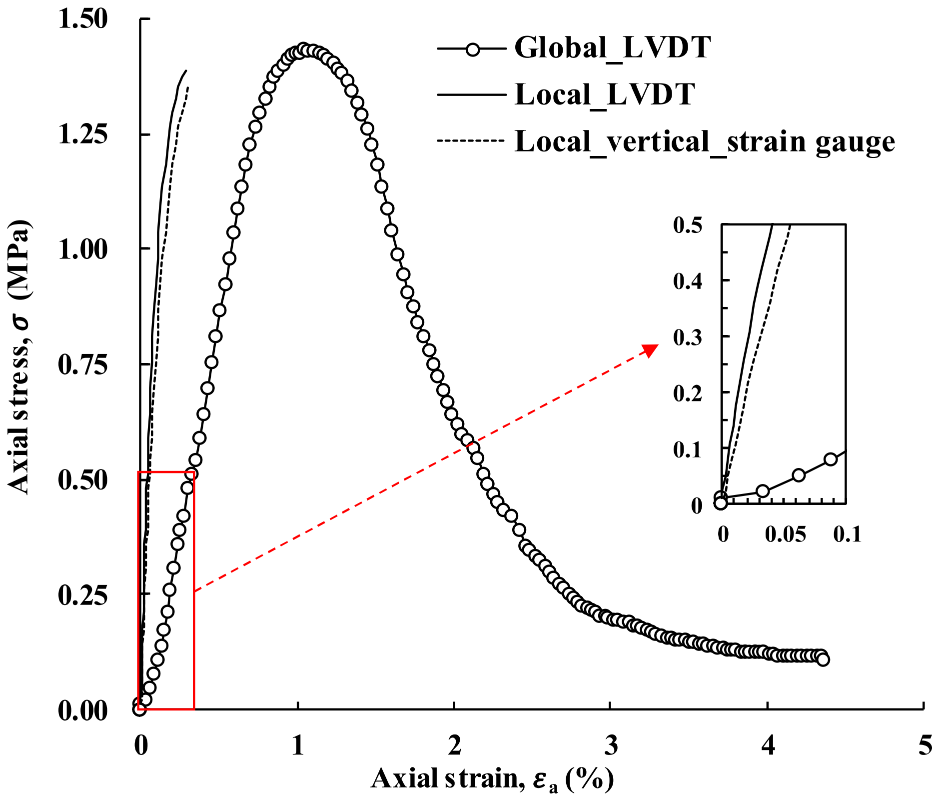

Fig. 2. A typical stress-strain curve of unconfined compression test on a cement stabilized HKMD specimen using global and local axial strain measurement methods

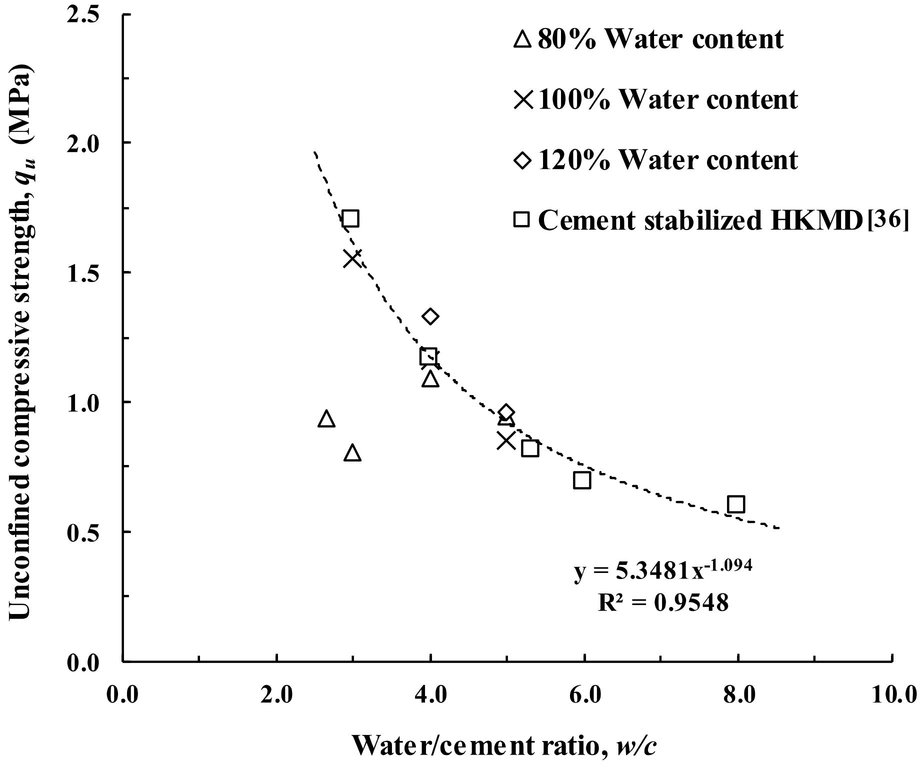

Fig. 3 Plot of unconfined compressive strength of cement stabilized HKMD versus water/cement ratio

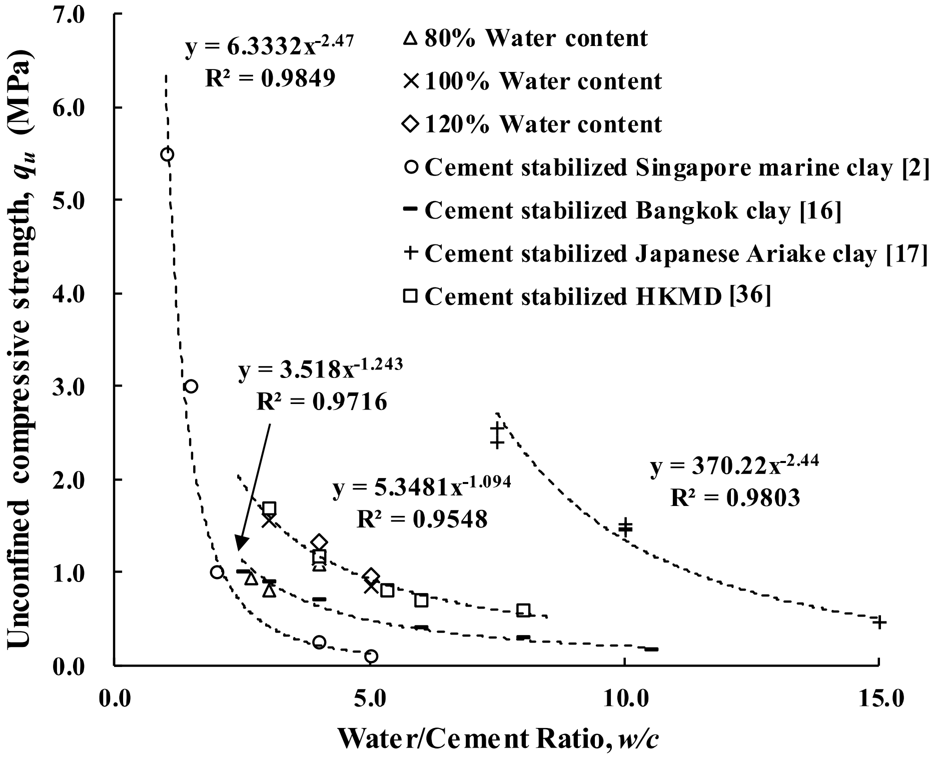

Fig. 4. Relationships between unconfined compressive strength of cement stabilized soils with water/cement ratio from different countries

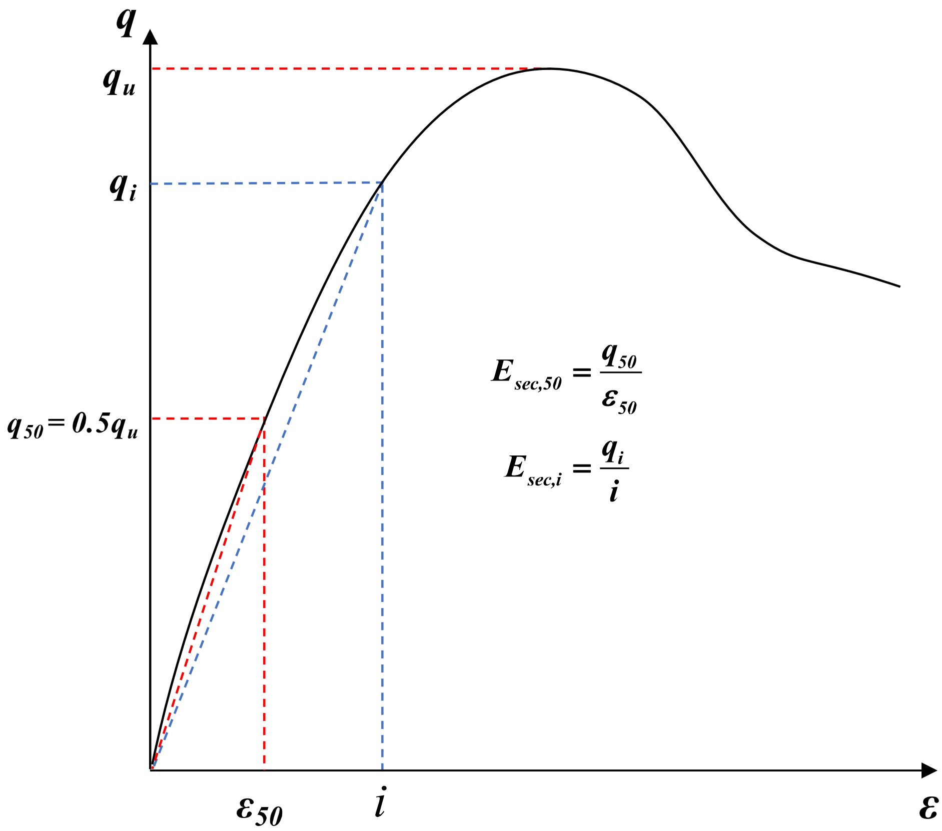

Fig. 5. A schematic diagram of methods for calculating of $E_{sec,50}$ and $E_{sec,i}$ from stress-strain curve

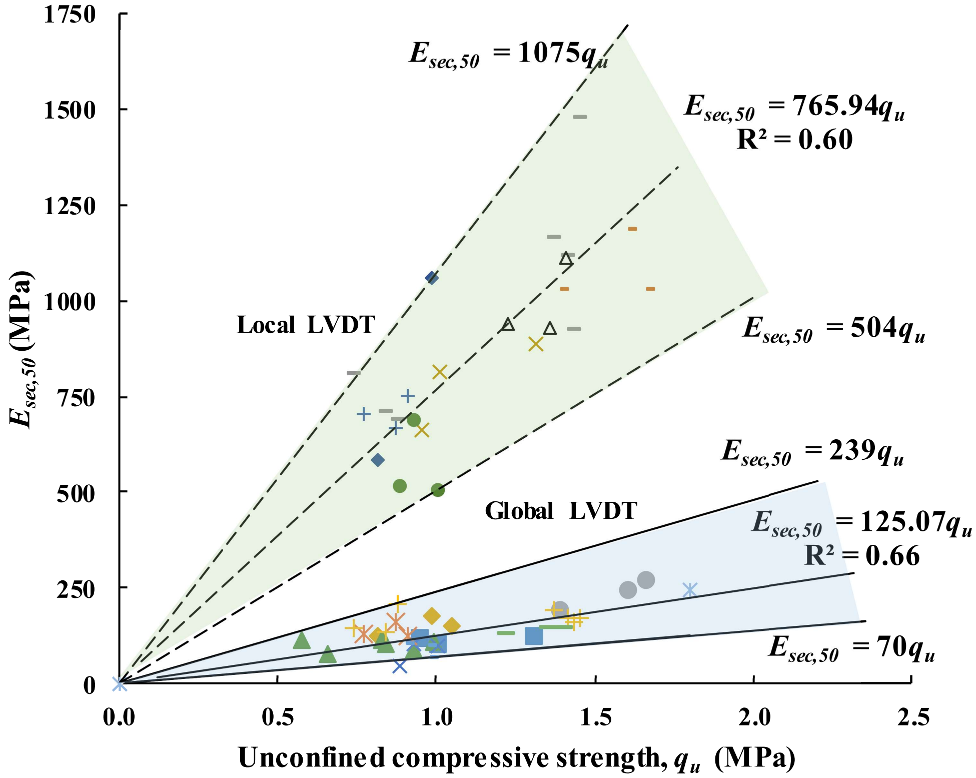

Fig. 6. Plots of unconfined compressive strength *versus* $E_{sec,50}$ determined by using local and global axial strain measurement methods

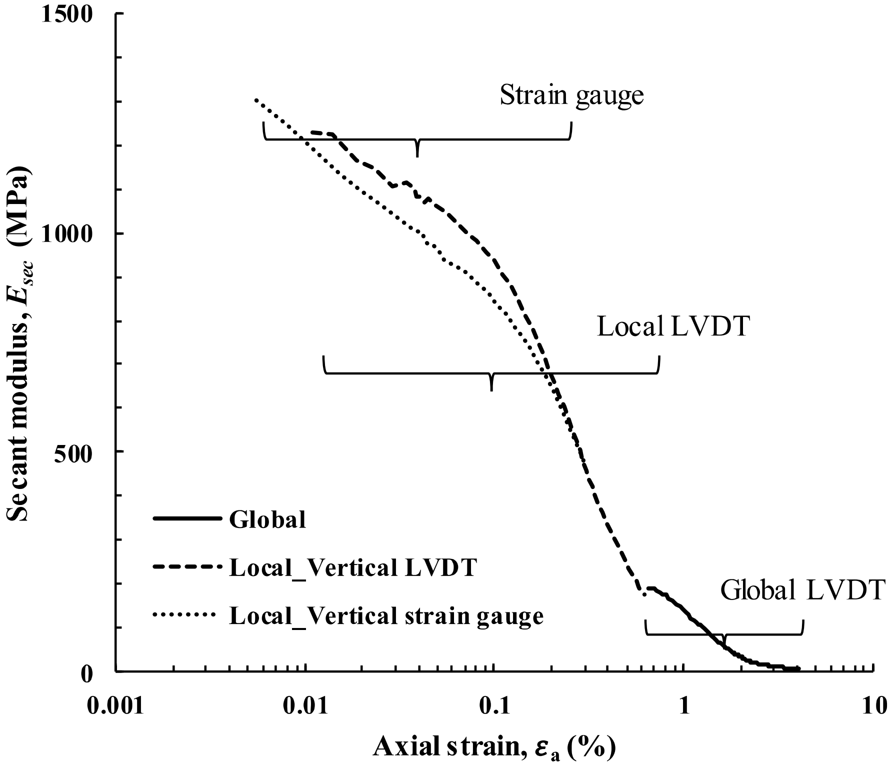

Fig. 7. Typical secant modulus degradation curve based on the data from global and local axial strain measurement methods

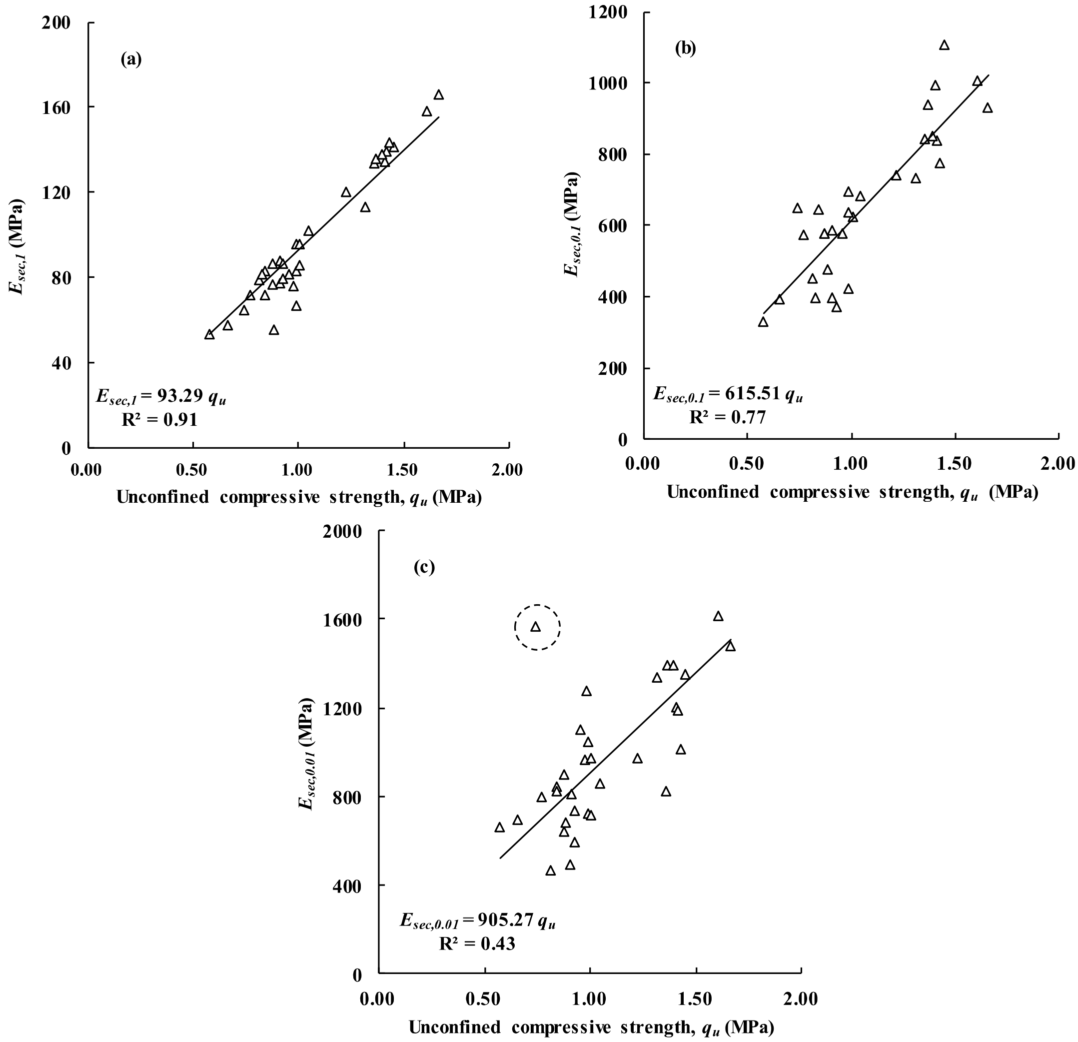

Fig. 8. Plots of secant modulus (a) $E_{sec,1}$, (b) $E_{sec,0.1}$, and (c) $E_{sec,0.01}$ of specimens with its corresponding unconfined compressive strength, q_u

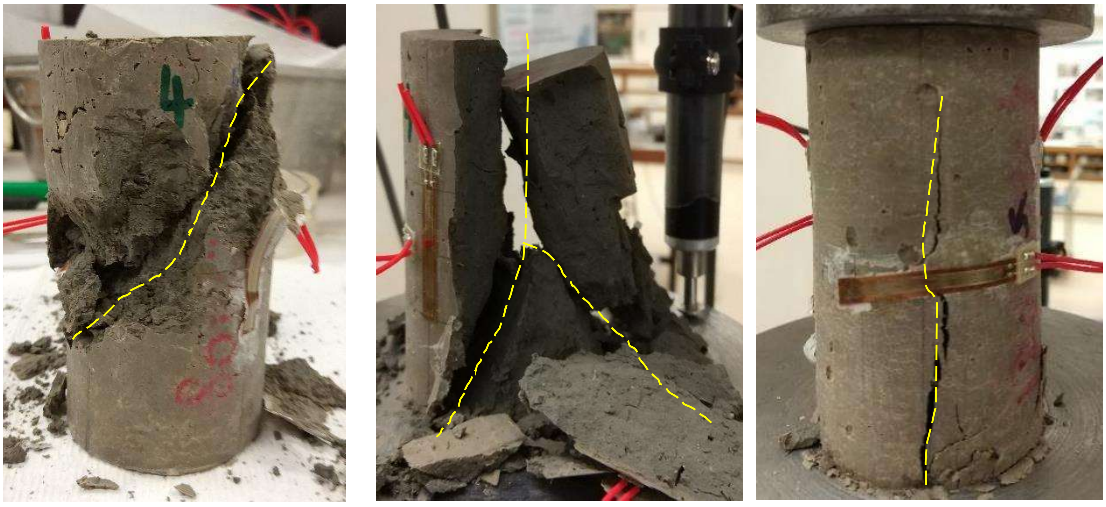

(a) Shear fracture W80_wc 2.67_3 | **(b) Cone and split fracture W100_wc 4_4** | **(c) Columnar fracture W120_wc 5_1**

Fig. 9. Typical failure modes of cement stabilized HKMD specimens: (a) shear fracture, (b) cone and split fracture, (c) columnar fracture

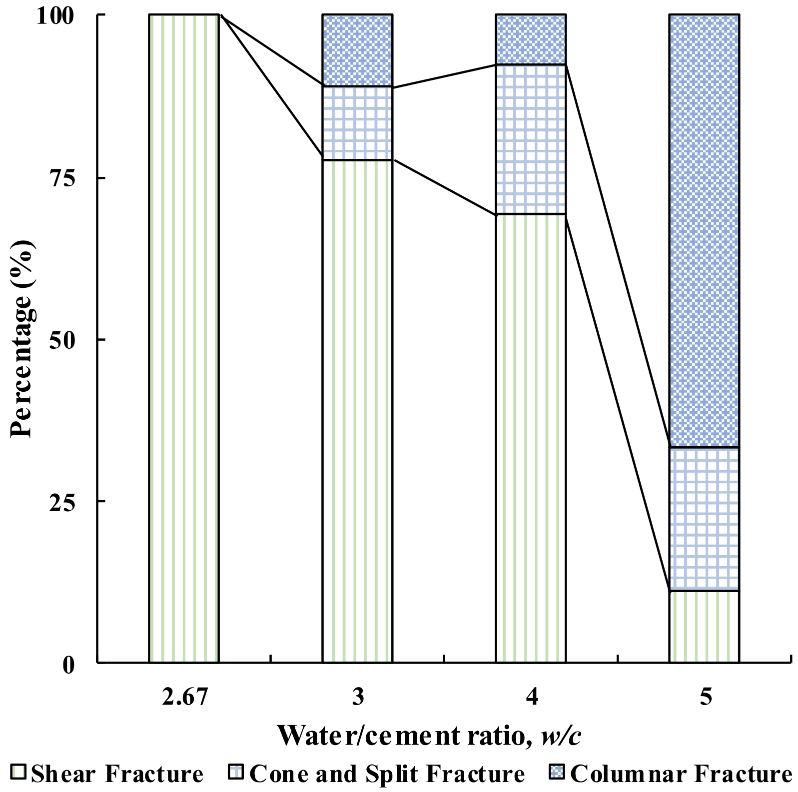

Fig. 10. Percentage of different failure modes of cement stabilized HKMD specimens with different *w/c* ratios

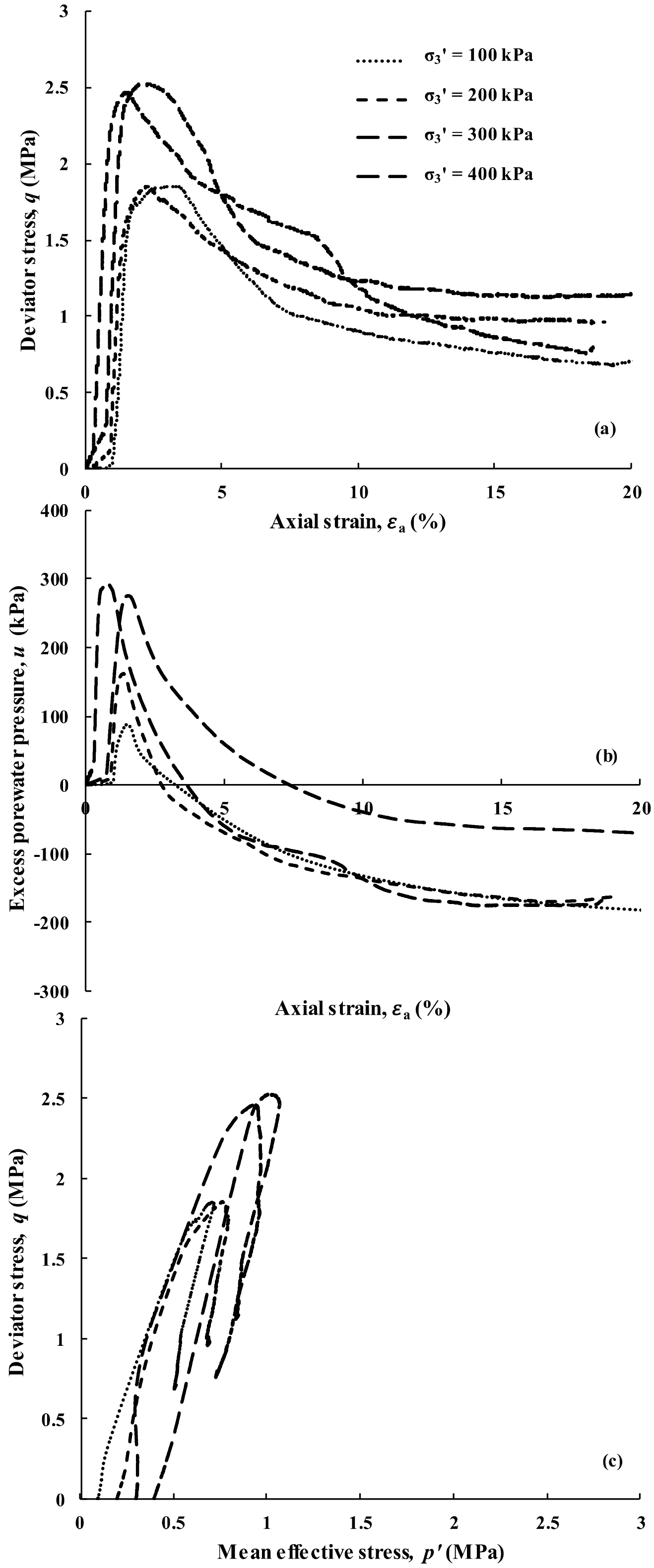

Fig. 11. Plots of (a) deviator stress *versus* aixal strain, (b)excess porewater pressure *versus* axial strain,(c) effective stress paths in compression stage of the specimens with 25% cement content and 100% water content (*i.e. w/c*: 4) under different confining pressures

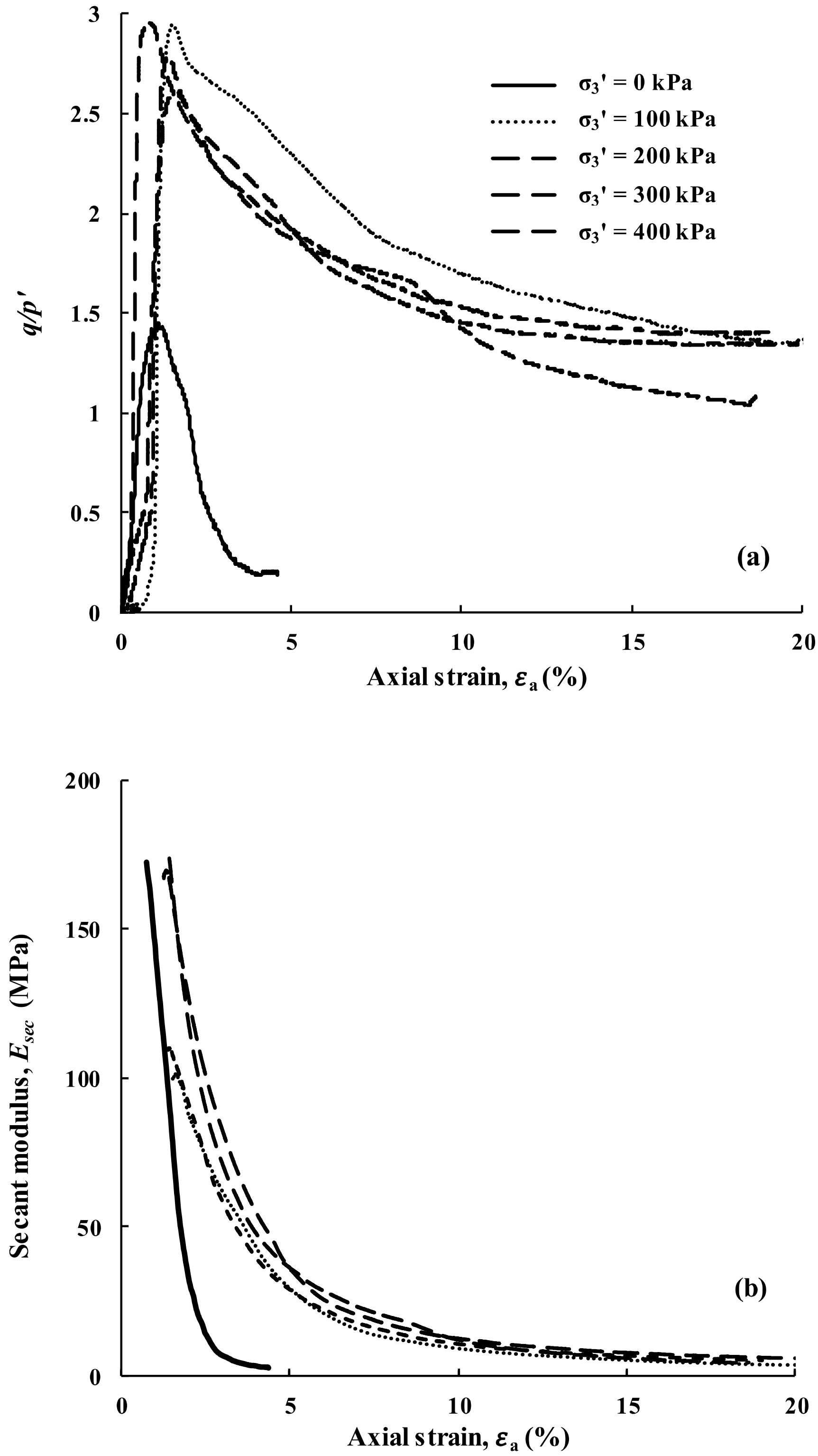

Fig. 12. Plots of (a) normalized stress-strain curve and (b) secant modulus *versus* axial strain of the cement stabilized HKMD specimen with 25% cement content and 100% water content (*i.e. w/c*: 4)